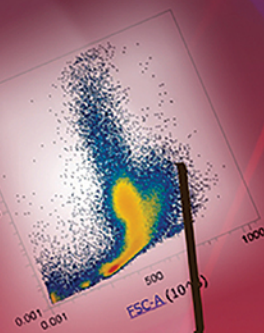
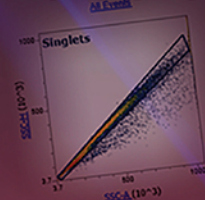
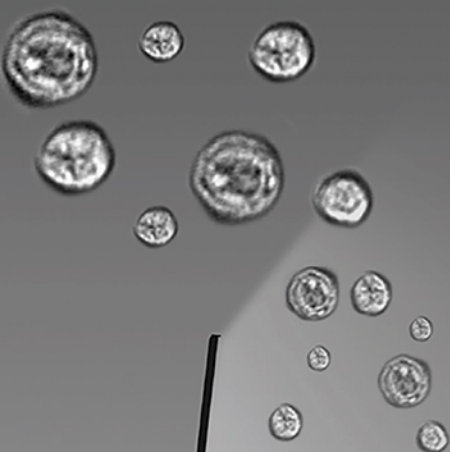


invitrogen

Two data sets. One step. Zero doubt.



Confidently confirm your cell profiles with a new flow cytometer that delivers flow cytometry and imaging data simultaneously. Now, you can acquire dual data quickly and easily. The new Invitrogen™ Attune™ CytPix™ Flow Cytometer delivers both brightfield images and flow cytometry data sets simultaneously, so you can confirm cellular characteristics and sample quality confidently, without changing your protocols.




Enhance analysis and confidence at [thermofisher.com/cytpix](https://www.thermofisher.com/cytpix)

ThermoFisher
SCIENTIFIC

For Research Use Only. Not for use in diagnostic procedures. © 2021 Thermo Fisher Scientific Inc. All rights reserved. All trademarks are the property of Thermo Fisher Scientific and its subsidiaries unless otherwise specified. COL25211 0621

Research Article

CD4⁺ T cells regulate glucose homeostasis independent of adipose tissue dysfunction in mice

Georg Brinker¹, Janine Froeba^{1,2}, Lilli Arndt², Julia Braune^{1,2},
Constance Hobusch¹, Andreas Lindhorst^{1,2}, Ingo Bechmann¹
and Martin Gericke^{1,2} 

¹ Institute of Anatomy, Leipzig University, Leipzig, D-04103, Germany

² Institute of Anatomy and Cell Biology, Martin-Luther-University Halle-Wittenberg, Halle (Saale), D-06108, Germany

Obesity is frequently associated with a chronic low-grade inflammation in the adipose tissue (AT) and impaired glucose homeostasis. Adipose tissue macrophages (ATMs) have been shown to accumulate in the inflamed AT either by means of recruitment from the blood or local proliferation. ATM proliferation and activation can be stimulated by TH2 cytokines, such as IL-4 and IL-13, suggesting involvement of CD4-positive T cells in ATM proliferation and activation. Furthermore, several studies have associated T cells to alterations in glucose metabolism. Therefore, we sought to examine a direct impact of CD4-positive T cells on ATM activation, ATM proliferation and glucose homeostasis using an *in vivo* depletion model. Surprisingly, CD4 depletion did not affect ATM activation, ATM proliferation, or insulin sensitivity. However, CD4 depletion led to a significant improvement of glucose tolerance. In line with this, we found moderate disturbances in pancreatic endocrine function following CD4 depletion. Hence, our data suggest that the effect on glucose metabolism observed after CD4 depletion might be mediated by organs other than AT and independent of AT inflammation.

Keywords: adipose tissue · inflammation · lymphocytes · macrophages · obesity



Additional supporting information may be found online in the Supporting Information section at the end of the article.

Introduction

Obesity has become an increasing burden for health systems around the world and has led amongst others to an unrivaled upsurge of type 2 diabetes [1]. The socioeconomic and personnel efforts to tackle the consequences of the obesity epidemic have become enormous [2]. It is therefore pivotal to elucidate the molecular foundation of obesity in order to develop targeted therapies.

On a cellular level, obesity is associated with a chronic low-grade inflammation in the adipose tissue (AT) that is characterized by an accumulation of various immune cells, namely T cells, B cells, neutrophils, mast cells, and macrophages [3–7]. This inflammation is most pronounced in the visceral adipose tissue (VAT), which is believed to have a more detrimental effect on metabolism than subcutaneous adipose tissue (SAT) [8,9]. Macrophages constitute the largest proportion of immune cells in the AT of obese rodents and humans respectively [3], and the extent of the accumulation of macrophages in the AT seems to be closely correlated to the degree of insulin resistance [10]. Macrophages occur in a continuum of different phenotypes from which two types are generally discerned: M1 macrophages are

Correspondence: Prof. Martin Gericke
e-mail: martin.gericke@medizin.uni-halle.de

induced by pro-inflammatory cytokines such as IFN- γ and express CD11c as a surface marker [11, 12]. In contrast, activation of M2 macrophages occurs in a TH2-related microenvironment, particularly due to IL-4 and IL-13, and leads to expression of CD206 and CD301 [11, 12]. Both populations seem to increase in number in the AT during obesity, but there is a marked increase in the proportion of M1 macrophages [13], which are located preferentially around dead adipocytes, in so-called crown-like structures (CLS). Further, it has been shown that the accumulation of adipose tissue macrophages (ATMs) during obesity occurs either by means of monocyte recruitment from the blood or proliferation of resident ATMs [14]. We and others have recently shown that the number of proliferating ATMs increases during obesity [15–17] and that this proliferation is at least partially mediated by cytokines such as IL4, IL13, and osteopontin (OPN), which are related to CD4-positive T helper cells (TH2 cells) [18–20]. This observation might suggest a link between macrophage activation and proliferation and CD4-positive TH2 cells.

CD4-positive T cells belong to the network of adaptive immune cells, which seem to play an important role in obesity-induced inflammation and insulin resistance [21]. To what extent the effect of lymphocytes on metabolism is immediate or mediated by macrophages and other immune cells is not known. Studies on mice with a RAG1 knockout, which abrogates the rodents capacity to produce any type of lymphocyte, have shown worsening of metabolic parameters, suggesting a protective role of lymphocytes [5]. It is assumed that the phenotype and function of lymphocytes alter during the course of obesity, leading to a loss of their protective properties. In line with this, depletion of CD3-positive T cells, CD20-positive B cells, and CD8-positive T cells in HFD-fed mice have shown attenuation of AT inflammation and improvement of metabolic parameters [4, 5, 22]. More accurately, depletion of CD3-positive T cells led to a marked upregulation of CD206-expressing ATMs while leaving adipocyte diameter unchanged. Likewise, depletion of CD8-positive T cells resulted in a decrease of CD11c-positive ATMs and a significant decrease of CLS formation. Both studies hence bring to attention the association between T-cell-mediated changes in glucose metabolism on one side and T-cell-mediated changes in VAT microenvironment on the other [5, 22]. The effect of an in vivo CD4 cell depletion on AT inflammation and glucose homeostasis during obesity is as yet undescribed, although it has been suggested that certain distinct CD4-positive cell populations might contribute to immune-mediated alterations in AT inflammation and glucose metabolism [20, 23]. Among these, VAT regulatory T cells (Tregs) have recently gained considerable attention for their potential to regulate AT and metabolic homeostasis [24]. In line with this, numerous studies have demonstrated that in situ expansion of Treg population in VAT led to attenuation of AT inflammation and improvement of glucose metabolism [23–27]. Importantly, in vivo loss-of-function models of VAT Tregs failed to show an effect on glucose metabolism in HFD-fed mice [24, 28–30].

CD4 cells, analogous to other immune cells in the AT, seem to increase in absolute numbers during obesity, yet inconsistencies exist as for the proportional changes: Some authors argue

for a relatively stable CD4 population [31], whereas others suggest a proportional diet-dependent decrease of CD4 cells in the course of obesity [5, 22]. Evidence further points towards a phenotypic switch among CD4 cells in the inflamed AT with a growing IFN- γ -positive population [5, 31] and a loss of forkhead box P3 (FOXP3) and suppression of tumorigenicity 2- (ST2) positive cells during obesity [30, 32, 33]. Both FOXP3 and ST2 are generally believed to have anti-inflammatory properties in the context of obesity-induced inflammation and various experiments suggest a beneficial effect on glucose metabolism [23, 25, 33–35]. The loss of these cells hence suggests the notion of a CD4 population that acquires a detrimental effect on glucose metabolism during the development of obesity.

The present work sought to elaborate further on the *modus operandi* of CD4-positive cells in the AT and aimed to elicit a possible impact on ATM activation and proliferation. We therefore established 3-day and 2-wk CD4 depletion protocols to evaluate short-term and potentially more direct changes as well as long-term effects on changes to the microenvironment. We show that short-term and long-term CD4 depletion have no apparent influence on either macrophage activation or macrophage proliferation in the AT, yet seem to have an impact on glucose homeostasis as measured by glucose tolerance testing (GTT). Furthermore, we show that long-term depletion of CD4-positive T cells causes dysregulation of the pancreatic endocrine axes, possibly contributing to the altered glucose metabolism following CD4 depletion. We conclude that in our study systemic CD4 depletion was shown to have no apparent effect on either CLS formation, ATM proliferation, or activation, yet entailed beneficial glucose tolerance potentially due to reasons beyond effects on VAT inflammation.

Results

CD4-positive T cells show time- and diet-dependent changes in the inflamed AT

First, we performed immunofluorescence staining of CD3- (Fig. 1B) and CD4+ (Fig. 1C) positive T cells to establish their presence and evaluate their distribution in the murine AT. We observed that CD3- and CD4-positive cells were mainly present in the CLS. Using flow cytometry, we then aimed to phenotype the CD3-/CD45-positive T cell population into their CD4- and CD8-expressing subsets. Therefore, we analyzed VAT of mice fed either an HFD or an NCD for 4, 12, or 24 wks. We detected a significant proportional increase of CD4-positive cells over time and independent of diet (Fig. 1A). At 24 wks, the proportion of CD8-positive cells was significantly larger in HFD-fed compared to control animals. This diet-dependent difference was absent in the overall proportion of CD4 cells (Fig. 1A). However, further phenotyping of the CD4-positive subset revealed significant diet-dependent changes of CD4 subsets. IFN- γ -positive CD4 cells significantly dropped at 12 wks and then seemed to increase after 24 wks in the HFD-fed animals (Fig. 1D). In contrast, expression of both Treg-associated FOXP3 and TH2-associated ST2 among

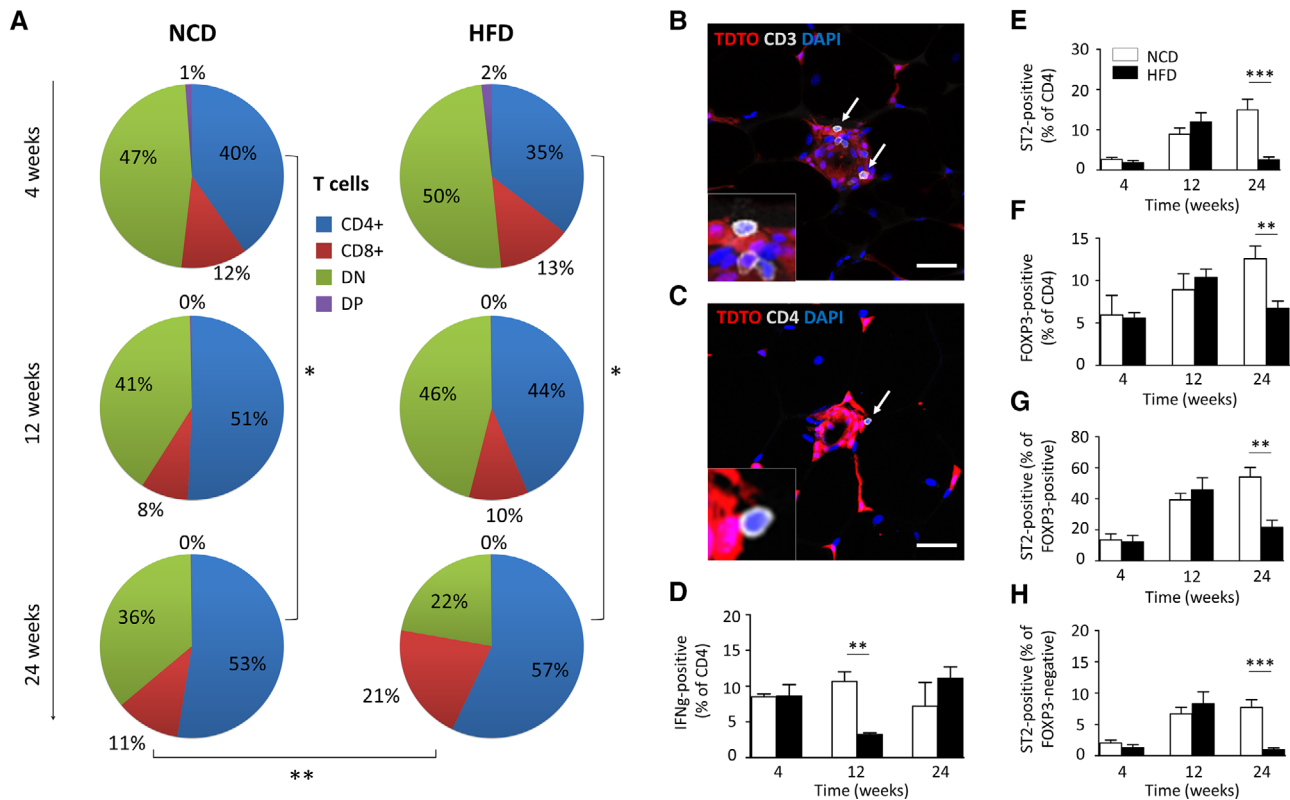


Figure 1. Immuno-profiling of adipose tissue lymphocytes (ATLs). (A) Flow cytometric analysis of CD4 and CD8 expression on ATLs in lean ($n = 4-6$) and obese ($n = 4-7$) mice on a C57BL6 background at 4, 12, and 24 wks. CD4-positive, CD8-positive, double-positive (DP), and double-negative (DN) subsets are depicted as proportion of CD3⁺CD45⁺ cells. Data come from eight experiments with two to six mice per experiment. (B and C) VAT of TDTO reporter mice was stained for CD3 (B; $n = 3$) and CD4 (C; $n = 3$) and DAPI. TDTO is expressed in macrophages and fluoresces red. In representative images of CLS, CD3 and CD4 fluorescence are shown in grey. Data are representative of two experiments with three mice per experiment. (D-H) Flow cytometric immuno-profiling for expression of IFN- γ , ST2, and FOXP3 among CD4-positive ATLs of mice fed either an NCD (white; $n = 5-10$, cumulative data from more than five independent experiments) or an HFD (black; $n = 5-10$; cumulative data from more than five independent experiments) for 4, 12, or 24 wks. Data are presented as column bar graphs and as means \pm SEM and were tested for statistical significance by Mann-Whitney U-test. * $p < 0.05$. ** $p < 0.01$. *** $p < 0.001$. Scale bar represents 50 μ m.

CD4-expressing lymphocytes showed a marked increase until 12 wks in both groups followed by a further increase in NCD-fed mice and a decrease in HFD-fed mice (Fig. 1E and F). At 24 wks, expression of both ST2 and FOXP3 were significantly lower in the HFD-fed group compared to NCD-fed controls (Fig. 1E and F). This reduced ST2 expression in obese mice at 24 wks was observed in both FOXP3-positive and FOXP3-negative cells, but was more pronounced in the FOXP3-negative population (Fig. 1G and H).

Three-day depletion of CD4-positive cells does not alter ATM activation or proliferation

To study the direct impact of CD4 cells on AT inflammation, we established a 3-day depletion protocol. CD4-specific antibodies were shown to efficiently deplete CD4-positive T cells by $\sim 99\%$. We further showed that depletion of CD4-positive T cells was consistent in both adipose and splenic tissue (Fig. 2C and D). Further, depletion did not result in significant weight loss averaging ~ 1 g in both groups after 3 days of depletion (data not shown).

After HFD-feeding for 24 weeks and antibody treatment according to protocol, we analyzed the AT phenotype. Fat cell expansion and formation of CLS are signs of tissue remodeling under high-caloric diet and could be observed in all animals (Fig. 3A and B). However, AT morphology as measured by adipocyte diameter did not alter between T-cell-depleted mice and mice treated with an appropriate isotype control (Fig. 3E). In order to evaluate AT inflammation, we counted the number of CLS in relation to adipocytes, which also revealed no significant difference (Fig. 3F). Another marker for the progression of AT inflammation is the proportion of ATMs among all stromal vascular cells. Again, no difference was observed (Fig. 3H). ATM activation as measured by the ratio of CD11c-positive ATMs (classically activated or M1 macrophages) in relation to CD206-expressing ATMs (alternatively activated or M2 macrophages) was quantified using flow cytometry and showed no effect under CD4 cell depletion (Fig. 3I). We then went on to assess a possible impact of CD4 depletion on ATM proliferation. First, we stained VAT for the proliferation marker proliferating cell nuclear antigen (PCNA; Fig. 3C and D). Since CLS have been shown to be the primary site of ATM proliferation, we focused our analysis on cells

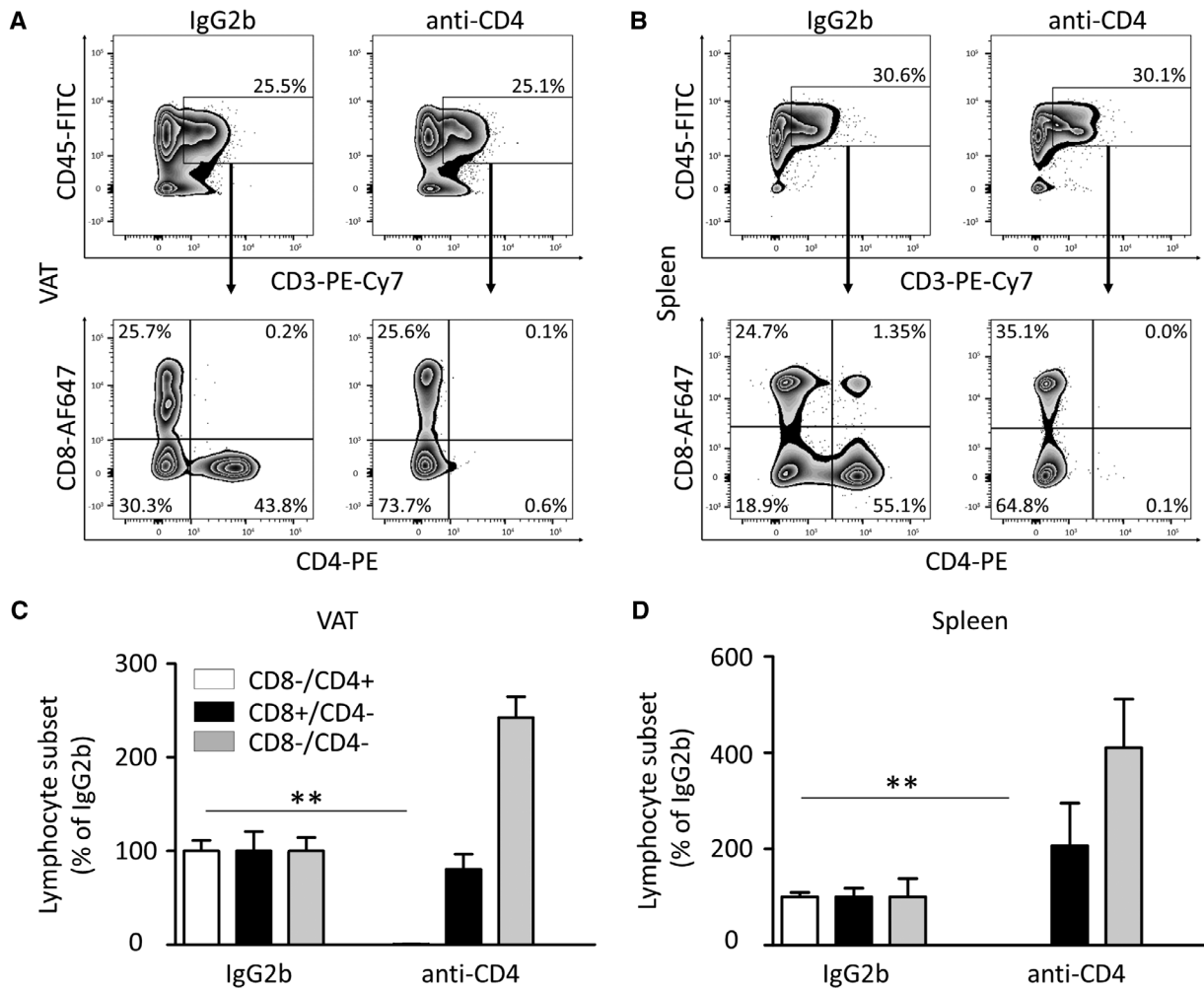


Figure 2. Flow cytometric analysis of T cell depletion in VAT and spleen. Efficiency of T cell depletion was assessed using flow cytometry. Cells were stained for the lymphocyte markers CD45, CD3, CD4, and CD8 prior to analysis. (A and B) Representative flow cytometry plots for the relative distribution of T cell subsets following depletion of CD4-positive cells or injection of an appropriate isotype control (IgG2b). (C and D) CD4-specific antibodies efficiently depleted CD4-positive T cells (white) by ~99% ($n = 4-6$ in both groups; cumulative data from 3 independent experiments). Depletion of CD4-positive T cells was consistent in VAT and spleen. Data are presented as means \pm SEM and as column bar graphs and were tested for statistical significance by Mann-Whitney U-test. ** $p < 0.01$.

residing within these structures. Quantification of immunohistochemistry showed no significant changes under CD4 cell depletion (Fig. 3G). Second, we performed flow cytometric analysis of Bromodeoxyuridine (BrdU) staining (Fig. 3J) that in accordance with the immunohistochemistry showed no significant difference between the groups. Likewise, mRNA levels of genes associated with ATM proliferation or activation showed no significant changes under CD4 cell depletion (Fig. 3K).

In the next step, we intended to compare the impact of CD4 cell depletion, as described above, with the effect of total T cell depletion. For that reason, we designed a similar 3-day depletion protocol for CD3 cells. However, we became aware that some mice in the CD3-depleted cohort showed signs of diarrhea and peritoneal inflammation in conjunction with a significant weight loss when compared with their IgG-injected control littermates (Fig. S2N). The depletion itself showed a moderate depletion efficiency

of ~66% in both spleen and VAT (Fig. S1). Importantly, ATM proliferation and activation remained unaffected by CD3 depletion (Fig. S2). Due to the observed weight loss and inflammatory changes, we concluded that the interpretation of our data was severely biased and decided to show these results in the supplementary section only.

Two-week depletion of CD4-positive cells does not alter ATM activation or proliferation

In order to rule out any indirect long-term effect of CD4-positive lymphocytes on ATM proliferation and activation, we established a 14-day depletion protocol. We then assessed AT integrity by means of immunohistochemistry as described in the previous section. Similar to the 3-day depletion experiment, AT morphology

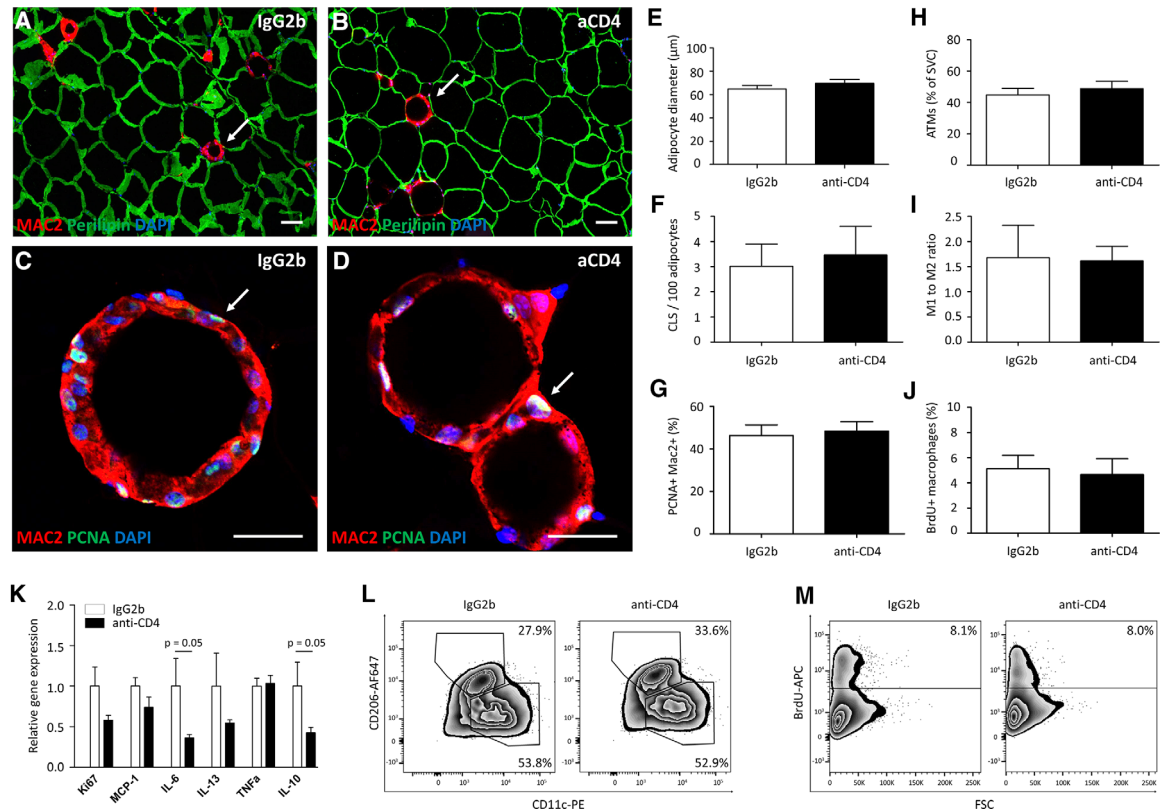


Figure 3. Effect of 3-day CD4 cell depletion on AT integrity. A and B, Representative images of immunofluorescence staining for the macrophage marker Mac2 (red), the fat cell marker Perilipin A (green) and DAPI (blue). White arrows show CLS. This immunofluorescence staining was used to quantify fat cell expansion (E) and density of CLS (F) (IgG2b cohort: $n = 8$, anti-CD4 cohort: $n = 10$; cumulative data from five independent experiments). (H–J) Flow cytometry was used to assess ATM density (H) ATM activation (I) and proliferation (J) (IgG2b cohort: $n = 4$ and anti-CD4 cohort: $n = 6$ in all experiments; each panel represents cumulative data from 3 independent experiments). For flow cytometric analysis of proliferation, AT stromal vascular fraction cells (SVC) were stained for BrdU. (C, D, and G) For morphological analysis of ATM proliferation, AT was stained for the macrophage marker Mac2 (red), the proliferation marker PCNA (green; white arrows in C and D) and DAPI (blue) (IgG2b cohort: $n = 8$, anti-CD4 cohort: $n = 10$; panel G represents cumulative data from five independent experiments, representative images are shown in panel C and D). (K) Whole AT gene expression analysis of Ki67 and various ATM proliferation- and ATM activation-associated cytokines was performed in IgG2b ($n = 3–4$) and anti-CD4 ($n = 5–6$) treated mice using quantitative real-time PCR (cumulative data from 3 experiments). Gene of interest mRNA levels were measured in duplicate and normalized to TBP. (L and M) Representative flow cytometry plots for M1/M2 and BrdU staining after treatment with IgG2b or CD4 antibody respectively (data analysis is shown in I and J). Data are presented as means \pm SEM and as column bar graphs and were tested for statistical significance by Mann–Whitney *U*-test. All scale bars represent 25 μ m.

showed no marked difference after 14 days of CD4 depletion compared to the isotype control (Fig. 4A and B). Likewise, adipocyte diameter and CLS density did not differ significantly between CD4-depleted and control mice (Fig. 4E and F). Quantification of proliferation by means of PCNA staining (Fig. 4C, D, and G) and by means of flow cytometry (Fig. 4J) also showed no alteration between the two groups, as did the proportion of ATMs and M1 to M2 ratio (Fig. 4H and I). Finally, the study of mRNA associated with ATM proliferation and activation revealed no significant changes in T-cell-depleted murine AT (Fig. 4K–N).

Glucose tolerance is improved under CD4-specific antibody treatment

In the next step, we aimed to determine any effect of CD4-specific antibody treatment on glucose metabolism. We therefore

performed GTT and ITT as described above. Interestingly, during GTT we observed significantly lower glucose levels at 30 and 120 min after glucose injection among the T-cell-depleted mice compared to mice treated with an appropriate isotype control (Fig. 5A). To evaluate the metabolic relevance, we performed area-under-the-curve analysis which also showed a significant difference between the two groups (Fig. 5B), suggesting a beneficial effect of CD4 cell depletion on glucose tolerance. During insulin tolerance testing we observed a mild, yet not significant, trend towards improvement of insulin tolerance under CD4 depletion (Fig. 5C and D).

Pancreatic endocrine function is altered following CD4 depletion

Finally, we sought to elaborate on a possible contribution of the pancreas to the observed difference in glucose metabolism.

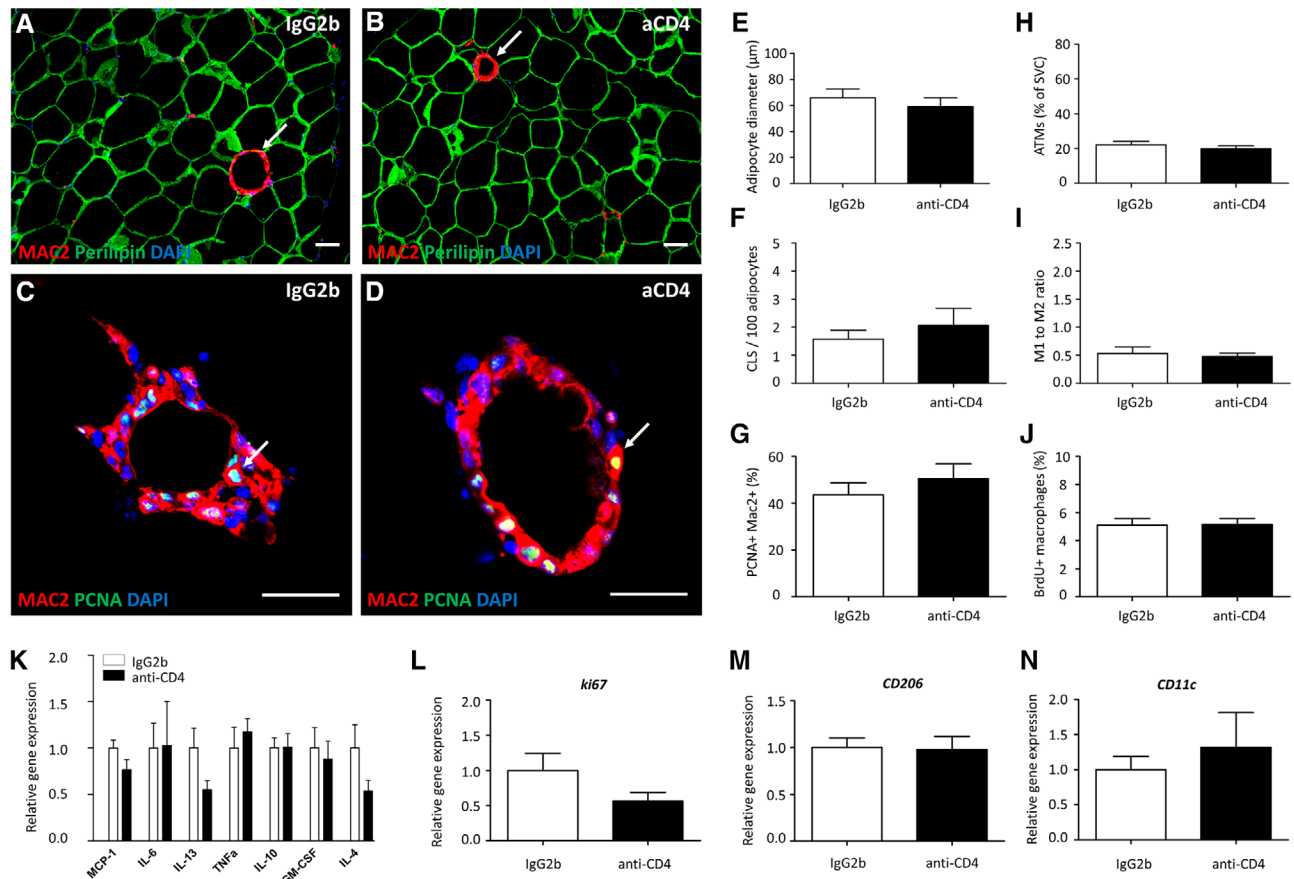


Figure 4. Effect of 14-day CD4 cell depletion on AT integrity. (A and B) Triple immunofluorescence staining of VAT for the macrophage marker Mac2 (red), the fat cell marker Perilipin A (green) and DAPI (blue) (representative images, data analysis shown in E and F). White arrows show CLS. (E and F) Quantification of Perilipin/Mac2 staining as measured by adipocyte diameter (E; $n = 6$ per group; cumulative data from 3 independent experiments) and number of CLS per 100 adipocytes (F; $n = 6$ per group; cumulative data from three independent experiments). (C and D) Triple immunofluorescence staining of VAT for the macrophage marker Mac2 (red), the proliferation marker PCNA (green; white arrows in C and D), and DAPI (blue) (representative images, data analysis shown in G). (G) Analysis of PCNA staining for ATM proliferation ($n = 6$; cumulative data from three independent experiments). (H–J) Flow cytometric quantification of ATM density (H; both groups $n = 8$), activation (I; both groups $n = 8$), and proliferation (J; both groups $n = 10$) (each panel represents cumulative data from five independent experiments). (K–N) Data from whole AT gene expression analysis using quantitative real-time PCR (both groups $n = 6$, cumulative data from three independent experiments). Gene of interest mRNA levels were measured in duplicate and normalized to TBP. Data are presented as means \pm SEM and as column bar graphs and were tested for statistical significance by Mann–Whitney *U*-test. All scale bars represent 25 μ m.

Morphometric analysis of pancreatic tissue as measured by islet quantity and size (Fig. 6B and C, representative images in Fig. 6A) revealed no significant alterations in mice injected with CD4-depleting antibody. However, frequency distribution analysis revealed a significantly higher proportion of very small islets (40–60 μ m) in pancreata of CD4-depleted mice (Fig. 6D). We then aimed at assessing the pancreatic endocrine function under CD4 depletion. Interestingly, fasting plasma insulin appeared to be similar between the two groups (Fig. 6E). Likewise, pancreatic insulin content was unchanged following CD4 depletion (Fig. 6G). In contrast, we observed a significant decrease in whole pancreatic content of glucagon (Fig. 6H). Further, protein analysis normalized to the islet protein content, as measured by GLUT2, also revealed a relative increase of somatostatin (Fig. 6I).

Discussion

The role of T cells in AT inflammation has been extensively studied over the past two decades. Two major *in vivo* depletion studies have suggested a substantial effect of adipose tissue lymphocytes (ATLs) on AT integrity and glucose homeostasis: CD3 depletion was shown to reduce M1 and increase M2 ATMs in VAT and positively influence glucose homeostasis [5]. Likewise, depletion of CD8-positive T cells resulted in an increased M2/M1 ratio in VAT, a reduction in CLS density, and beneficial effects on insulin sensitivity and glucose tolerance [22]. These two studies both suggest that ATLs acquire a pro-inflammatory phenotype during high-fat feeding, depletion of which partially restores the disrupted AT integrity and attenuates the impaired glucose metabolism in HFD-fed mice. In this study, we aimed to substantiate this claim by

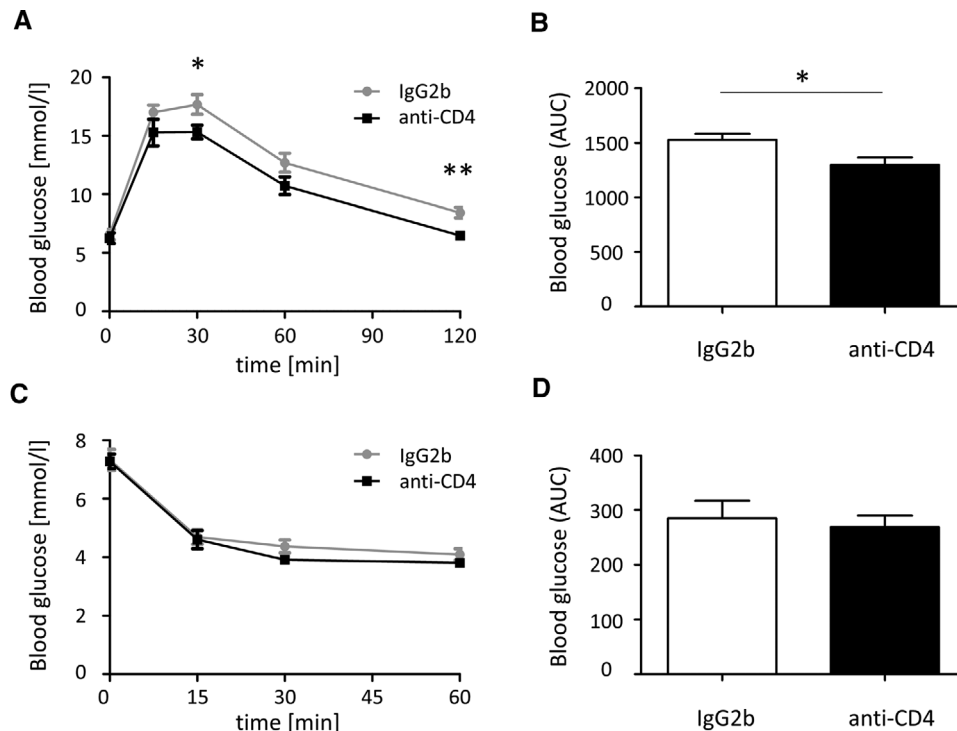


Figure 5. Impact of 14-day CD4 cell depletion on glucose homeostasis. (A) Glucose tolerance testing (GTT) on mice treated with CD4-depleting or IgG2b control antibodies for 14 days after 24 wks of HFD-feeding ($n = 10$ per group; cumulative data from 5 independent experiments). (B) Area-under-the-curve (AUC) analysis of GTT. (C) Insulin tolerance testing (ITT) on mice treated with CD4-depleting or IgG2b control antibodies for 14 days after 24 wks of HFD-feeding ($n = 10$ per group; cumulative data from 5 independent experiments). (D) Area-under-the-curve analysis of ITT. Data are presented as means \pm SEM and were tested for statistical significance by unpaired t-testing, * $p < 0.05$. ** $p < 0.01$.

elucidating the effects of CD4-positive T cells on AT inflammation and glucose homeostasis.

There are conflicting propositions in the literature, first, as to the sequence of events regarding T cell involvement and, second, as to the extent of quantitative and qualitative changes in the VAT T cell population. Studies using mRNA as a target have suggested a relatively early expansion of CD3-positive cells in HFD-induced inflammation that coincides with changes in glucose homeostasis and precedes macrophage expansion [36, 37]. It has been argued that this early expansion of CD3-positive cells in VAT is limited to the CD8-positive subset whereas CD4-positive T cells decrease [5, 22]. However, other studies make the case for an early CD4 cell expansion [20] or a relatively stable CD4 population [31]. In our study, we demonstrate an age- but not diet-dependent proportional increase of CD4 cells in VAT and a numerically but not phenotypically stable CD4 population with regard to the impact of an HFD. Equally unclear is the role of IFN- γ -releasing CD4 cells with studies arguing for either an increase [5] or a reduction [38] of this population under the influence of HFD-feeding. Our results seem to concur with the latter, although we also detected an increase to lean levels at a later time point. Our data thus argue against a major impact of IFN- γ released by CD4 cells in the context of late AT inflammation. However, the highly significant drop of IFN- γ -releasing CD4 cells at 12 wks of HFD also described by Zamarron et al. [38] poses the question of different AT responses to high-caloric stimuli during

different time points and could instigate further research. Relative consensus exists as to the FOXP3-positive Treg population that seems to increase with age and decrease under high-caloric feeding [5,22,23,30,32] selectively in VAT but not splenic tissue or SAT [23]. A similar dynamic has been reported for ST2 expression on FOXP3-positive and FOXP3-negative T cells respectively [33]. Our data agree with this observation, leading us to argue for an obesity-induced decrease of FOXP3 and ST2 expression that is inverse to the age-related increase in chow-fed animals. ST2 and FOXP3 are generally considered to have anti-inflammatory properties in the context of obesity-induced inflammation [23,25,33–35].

Our results hence led us to believe that depletion of the CD4 population that has tilted towards a more pro-inflammatory phenotype would propel similar changes as seen with CD8 or CD3 depletion respectively. We therefore established a highly efficient 3-day and 14-day depletion protocol to account for short- and long-term effects on AT integrity. It should be noted that the mice cohorts used in both experiments differed quite significantly regarding their total body weight. However, the two experiments were not designed to be compared directly and both groups express a degree of AT inflammation that is distinct from AT morphology in lean animals. Interestingly, both depletion experiments showed no effect of depletion on adipocyte size, number of CLS, macrophage activation, or proliferation. We were able to reproduce these results using a short-term CD3 depletion protocol,

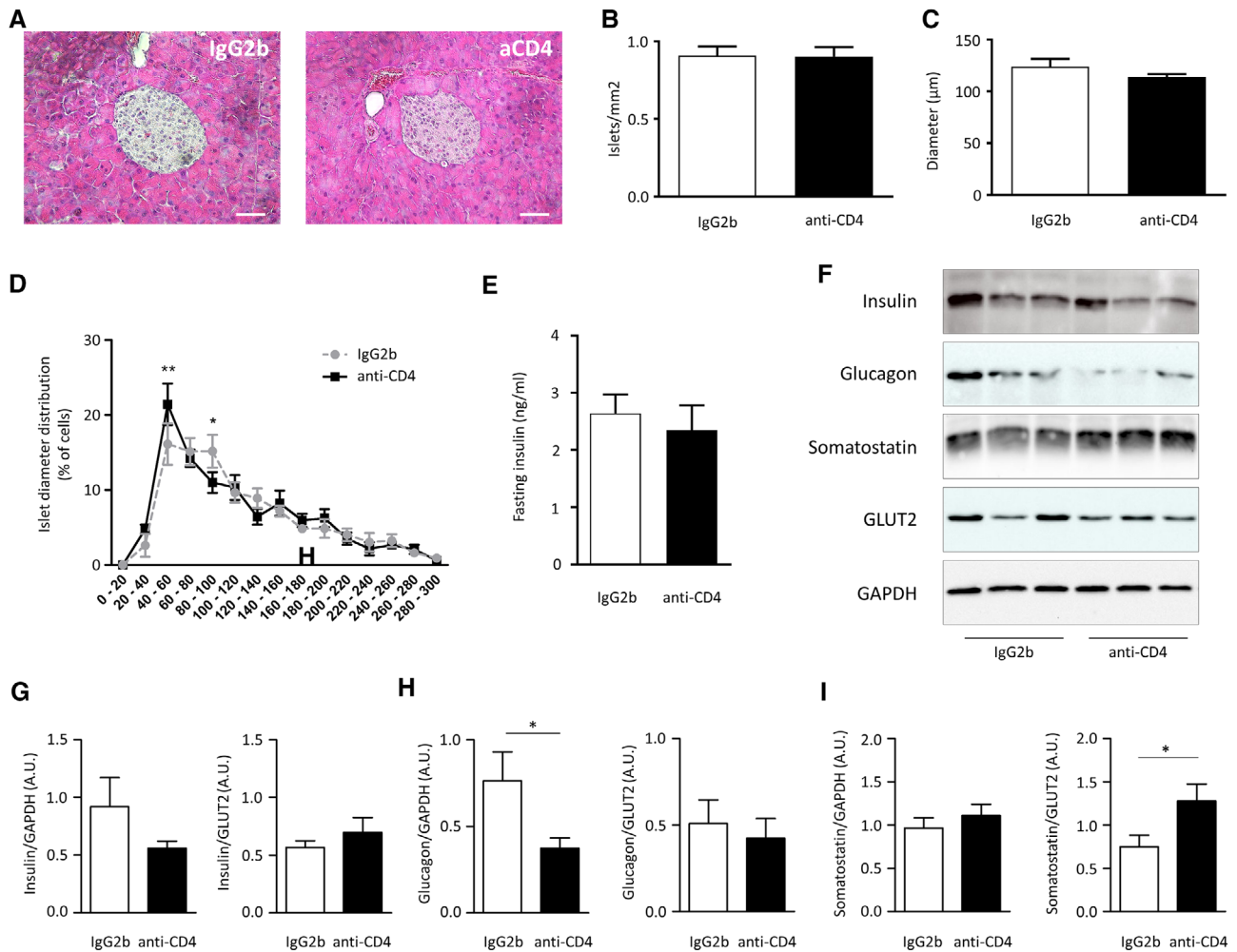


Figure 6. Impact of 14-day CD4 depletion on pancreatic tissue integrity and secretory function. (A) Hematoxylin and eosin staining of pancreatic tissue (representative images of islets, data analysis shown in B and C). (B and C) Morphometric analysis of pancreatic tissue as measured by number of islets per mm² pancreatic tissue (B; n = 6 per group; cumulative data from three independent experiments) and islet diameter (C; n = 6 per group; cumulative data from 3 independent experiments). (D) Frequency distribution analysis of islet size (shown as histogram with 20 μm bin width (n = 6 per group; cumulative data from three independent experiments)). (E) Fasting plasma insulin in mice treated with either CD4-depleting or control antibody was measured using ELISA (n = 8 per group; cumulative data from four independent experiments). (F) Representative Western blots of insulin, somatostatin, glucagon, GLUT2 and GAPDH following depletion of CD4-positive cells or injection of an appropriate isotype control. Uncropped Western blots can be found in Supporting Information Fig. 4. (G–I) The abundance of insulin (G; both groups n = 8), glucagon (H; both groups n = 8), and somatostatin (I; both groups n = 8) is normalized to both GAPDH to account for whole pancreatic cell mass and GLUT2 to account for islet cell mass (panel G, H, and I represent cumulative data from four independent experiments with four mice per experiment). Data are presented as means ± SEM and as column bar graphs and were tested for statistical significance by unpaired t-testing, *p < 0.05. **p < 0.01. Scale bar represents 50 μm.

however interpretation of the data was confounded by weight loss in depleted mice.

It should be acknowledged that weight loss has been reported in numerous studies using the CD3-depleting hamster IgG 145 2C11 [5, 39–43]. This has been attributed to a cytokine release syndrome triggered by activation of Fc receptors. However, in this study, we used the rat IgG 17A2 that has been explicitly demonstrated not to induce the same significant morbidity associated with the 145 2C11 antibody [42, 43]. The severe reaction of some of the mice in our anti-CD3 cohort was therefore unexpected. Caution in using and interpreting data obtained from CD3 depletion with both, 17A2 and 145 2C11, should therefore be advised.

However, for appropriate comparison between data after CD3 and CD4 depletion, a similar IgG-based approach has been used, which did not show any adverse effects in CD4 depleted mice.

We and others have recently described ATM proliferation as a characteristic of AT inflammation [16, 17], which seems to be dependent on cytokine stimulation namely by TH2-related cytokines IL-4, IL-13, and OPN [18, 19]. Furthermore, CD4 cells have been shown to be the main source of OPN in VAT [20]. However, various techniques used in this study to evaluate ATM proliferation have been consistent in showing no effect of CD4 depletion, leading us to believe that CD4 cells play a minor role in prompting ATM proliferation under high-caloric feeding.

CD4 depletion however seems to have some effect on glucose metabolism, since we showed significant improvement of GTT, but not ITT following CD4 depletion. This suggests some degree of impaired insulin production in reaction to glucose challenge but not insulin resistance *per se*. This discrepancy led us to hypothesize a potential pancreatic involvement. Both groups showed signs of islet hypertrophy, which have been described as characteristic of diet-induced obesity [44]. Yet, we failed to observe a significant difference in trophic conditions under CD4 depletion. Furthermore, we did neither detect an increase of insulin expression nor enhanced fasting insulin levels under CD4 depletion. Interestingly however, we observed a significant reduction of glucagon in the pancreatic tissue and a significant increase of somatostatin in proportion to islet cell mass in CD4-depleted mice, suggesting an impact of CD4 cells on alpha and delta cell homeostasis. Alpha-cell dysfunction has been described as a hallmark of type 2 diabetes [45, 46]. Indeed, hyperglucagonism was shown to be present in obese subjects in the fed and fasted state in numerous studies [47–50]. Furthermore, alpha cell dysfunction seems to result in an inability to suppress glucagon in reaction to glucose challenge [51–53]. Novel therapeutics rely partly on the antagonism of glucagon action [54]. The inadequate alpha cell output, in turn, appears to be counter-regulated by somatostatin [50,55]. It has been suggested that this effect is mediated by an absolute decrease in delta cell output and a loss of somatostatin sensitivity of alpha cells in the state of impaired glucose tolerance. [50, 56] Therefore, it might be reasonable to speculate that glucagon and somatostatin disturbance, as observed in our study, partly contribute to the beneficial metabolic phenotype exhibited by CD4-depleted mice. However, studying the pancreatic involvement was not the primary focus of this study and should therefore warrant further research.

Likewise, the beneficial effect of CD4 depletion on whole-body glucose tolerance is in agreement with the notion that CD4 cells acquire a phenotype that is detrimental to insulin sensitivity during the course of obesity. However, whereas CD3 and CD8 depletion seem to influence both glucose homeostasis and ATM activation, effects of CD4 depletion seem to be independent of such changes. Potentially these effects are mediated by cytokines that do not have a major impact on either ATM phenotype or proliferation.

That said, in the absence of an established method to selectively deplete organ-specific cells *in vivo* without prior genetic modifications, we currently rely on systemic depletion protocols, making it difficult to attribute an observed systemic effect to site-specific changes in the microenvironment. Such inherent limitations apply to all depletion studies and therefore it has to be highlighted that this study was not designed to provide a mechanistic insight into the origins of CD4-mediated effects on glucose metabolism and that the above-mentioned models postulating a pancreatic or VAT involvement in CD4-mediated changes in glucose tolerance are speculative in nature and do not rule out the potential involvement of other organs.

In conclusion, our results show that the CD4 cell population in VAT shifts towards a more pro-inflammatory phenotype and

that systemic depletion of CD4 cells improves glucose tolerance while leaving insulin sensitivity, AT morphology, ATM activation, and ATM proliferation as signs of AT dysfunction unaffected.

Material and methods

Experimental animals

Mice strains were kept in our local animal facility in a temperature-controlled, 12 h-light/dark cycle environment with ad libitum access to food and water. In order to induce obesity C57BL/6 mice were fed an HFD (60% kcal fat; Ssniff Spezialdiäten, Soest, Germany) or a normal chow diet (9% kcal fat; Ssniff Spezialdiäten) up to 24 weeks, starting at 6 weeks of age. For some experiments, CSF1R-eGFP^{+/−} (MacGreen; [57]) or LysMCre x TDTO^{flx/flx} [58] on a C57BL/6 background were used, depending on the spectral requirements. Of note, reporter mice develop an AT inflammation similar to wild-type C57BL/6 mice [59]. All studies used males and were approved by the local ethics committee (42502-2-1554 MLU).

Depletion

For depletion of CD4-positive cells, mice were injected with 120 μ l of anti-CD4 (GK 1.5; BioLegend, San Diego, CA) or an isotype control (RTK4530; BioLegend) using a 3-day protocol and a 2-wk protocol. With the 3-day depletion protocol, mice received either injection for 3 consecutive days. With the 2-weeks protocol, mice received 3 injections each week for 2 wks as described by Nishimura et al. [22]. ITT and GTT were performed at the end of the 2-wk depletion protocol only. Experiments were performed under specific pathogen free (SPF) conditions, following FELASA criteria. Importantly, mice after CD4 depletion were indistinguishable from control mice, without any signs of diarrhea, conjunctivitis, or a significant drop in body weight.

For depletion of CD3-positive cells, mice were injected with 120 μ l of anti-CD3 (17A2; BioLegend, San Diego, CA) or an isotype control (RTK4530; BioLegend) using a 3-day protocol as described above. Strikingly however, some mice showed signs of diarrhea and peritoneal inflammation in association with a considerable weight loss (Fig. S2N) following CD3 cell depletion, for which reason, we have decided to show the acquired data in the supplementary section only (Fig. S1 and 2).

ITT/GTT

For ITT, baseline glucose level was measured before mice were injected with insulin (Insuman Rapid, 100 IU/ml). Blood glucose was measured again at 15, 30, and 60 min after injection. Mice received 1.5 U/kg insulin solution intraperitoneally. ITT was performed 3 days prior to GTT. For GTT, mice were fasted for 12 h

prior to testing. Baseline sugar was measured prior to injection of glucose (20%; B. Braun, Melsungen, Germany). Glucose level was then measured at 15, 30, 60 and 120 min after injection. Mice received 1 g/kg glucose solution intraperitoneally.

Immunofluorescence

Mice were sacrificed and VAT was dissected. VAT was then fixed in zinc formalin overnight and embedded in paraffin. Paraffin sections were deparaffinized, microwaved, and washed in PBS with 0.3% Triton (PBST). Subsequently, unspecific binding sites were blocked using PBST and 1% BSA for 1 h at room temperature. AT was stained with primary antibodies at 4°C overnight. For AT analysis, AT was stained using the macrophage marker Mac-2 (CL8942AP; 1:1000; Cedarlane; Burlington, Canada) and the fat cell marker Perilipin A (ab3526; 1:200; Abcam, Cambridge, UK). For proliferation studies, macrophages were stained against Mac-2 and the proliferation marker PCNA (ab15497; 1:200; Abcam). DAPI (1:10,000; Thermo Fisher Scientific, Schwerte, Germany) was used for nuclear staining. Appropriate secondary antibodies were selected and incubated for 1 h at room temperature. For AT analysis, images were taken using the Olympus BX40 epifluorescence microscope. For proliferation studies, AT was studied using an inverted confocal microscope (FV1000 Olympus, Hamburg, Germany).

Analysis of AT sections

For AT analysis, the tissue was stained for Mac-2 and Perilipin A as described above. AT integrity was evaluated by measuring fat cell diameter and formation of CLS. CLS were defined as adipocytes entirely surrounded by leucocytes as described by others [60, 61]. CLS per field were counted in 10 randomly chosen fields on one section per animal. For the study of proliferating ATMs, staining for PCNA was performed as described above. ATMs were visualized by staining for Mac-2. Since it has been shown that up to 90% of ATMs in the inflamed AT reside in CLS [60] and proliferation was shown to occur predominantly in CLS [17], 20–30 photographs of CLS were taken per section and analyzed for content of proliferating cells.

Analysis of pancreatic tissue sections

For analysis of islet morphology, pancreatic tissue was stained with H&E. Subsequently, the area of pancreatic tissue was determined in three H&E-stained sections per animal (minimal distance 300 µm). Islets were counted in these sections (mean 76.8 ± 7.8 islets per mouse) and displayed as number per mm² of whole pancreatic tissue. Similarly, the diameter of islets was measured and averaged over all islets present in all three sections. Images were taken using a Keyence microscope (Neu-Isenburg; Germany).

Whole-mount staining

Whole mounts of AT from tdTomato (TDTO) reporter mice were used to visualize presence of CD3- and CD4-positive cells in AT. For that purpose, epididymal AT was immediately fixed after sacrifice for 20 min in zinc formalin (Polysciences, Hirschberg, Germany), washed in PBS, and cut into small pieces (<1 mm³). These AT pieces were then washed in PBS, blocked with staining buffer (3% BSA in PBS) for 1 h at room temperature, and stained with pre-labeled antibodies in staining buffer (anti-CD3-PE-Cy7; 1:100 145-2C11; BioLegend or anti-CD4-AF647; 1:100; RM4-5; BioLegend) overnight. We used Hoechst (1:10,000 in PBS; Life Technologies) to stain the nuclei. AT pieces were then washed three times in PBS and subsequently transferred into cavities of microscope slides and mounted using Fluorescence Mounting Medium (Dako; Hamburg; Germany). AT was studied using the Olympus FV1000 confocal microscope.

Flow cytometry

For flow cytometry analyses, VAT and spleen were dissected. VAT was digested with collagenase type II (Worthington Biochemical, Lakewood, NJ) centrifuged and the lipid phase discarded in order to gain a cell suspension of stromal vascular cells (SVCs). This suspension was then filtered through a 75 µm mesh. Splenic tissue was minced using a razor blade and pressed through a 70 µm mesh using a syringe plunger. Fc receptors of splenic cells and SVCs were blocked using anti-CD16/32 (1:100; eBioscience, Frankfurt, Germany) for 10 min on ice. Surface staining was performed using anti-CD45-FITC (30-F11; 1:100) or anti-CD45-APC-eFluor780 (30-F11, 1:200), anti-F4/80-PE-Cy7 (BM8, 1:100), anti-CD11c-PE (N418; 1:100; all eBioscience), anti-CD206-AF647 (MR5D3; 1:50; AbD Serotec, Kidlington, UK), anti-CD3-PE-Cy7 (145-2C11) anti-CD4-PE (RM4-5) or anti-CD4-AF647, (RM4-5), anti-CD8-AF647 (YTS156.7.7; all 1:100; all BioLegend), and anti-ST2-PE (RMST2-2; 1:100; eBioscience) for 20 min on ice. After fixation and permeabilization with the allophycocyanin (APC) BrdU flow kit (BD Pharmingen, Heidelberg, Germany) cells were again stained using anti-FOXP3-eF450 (FJK-16; 1:100; ThermoFisher), anti-IFN-gamma-PE (XMG1.2; 1:100; eBioscience), or anti-BrdU-Alexa Fluor 647 (PRB-1; 1:50; Abcam). For detection of BrdU, mice were injected with 200 µl BrdU 3 h prior to the experiment. After Fc-blocking, staining of surface markers, and fixation as described above, cells were further treated with DNase IV (Sigma-Aldrich, Deisenhofen, Germany). For IFN-γ detection, SVCs were cultured in RPMI 1640 medium (Sigma-Aldrich) supplemented with 10% fetal calf serum and 0.6% PSA (penicillin, streptomycin, und amphotericin B) at 5% CO₂/21% O₂ and 37°C. Later, leucocyte activation cocktail with BD GolgiPlug™ (BD Pharmingen) was applied according to the manufacturer's protocol and the cells were incubated overnight for 12 h. The following day, Fc-blocking, staining, and fixation were performed as described above. 7-Aminoactinomycin D (7-AAD; BD Pharmingen) was used for DNA

staining. Appropriate isotype controls were duly performed for all experiments. Analysis was performed using an LSR II (BD Pharmingen) equipped with FACSDiva software 8.0. Quantification of flow cytometry data was implemented using FlowJo software 10.0.5 (Tree Star, Ashland, OR). Gating strategies are described in detail in the supporting information (Fig. S3). Guideline for the use of flow cytometry studies was duly followed [62].

Gene expression analysis

Analysis of relative gene expression was performed using quantitative real-time PCR (Maxima SYBR Green quantitative PCR master mix; Thermo Fisher Scientific) on a Bio-Rad CFX96 Manager system (Bio-Rad, Munich, Germany). RNA was extracted (TRI Reagent solution; Thermo Fisher Scientific), followed by synthesis of cDNA using oligo (dT) primers and a ProtoScript first-strand cDNA synthesis kit (New England Biolabs, Frankfurt am Main, Germany). Gene-specific primers (presented in Supporting Information Table S1) were designed with the Primer 3 software. Gene of interest mRNA levels was measured in duplicate and normalized to TATA-binding protein (TBP). The acquired data were analyzed with the $\Delta\Delta C_t$ method by Pfaffl [63].

Enzyme-linked immunosorbent assay

Plasma concentrations of insulin were measured using ELISA according to the manufacturer's guideline (Mouse Insulin ELISA, ALPCO, Salem, USA).

Western blot analysis

Western blot was performed as described by others [64]. Total protein from pancreas samples were extracted using RIPA lysis and extraction buffer (Thermo Fisher Scientific) supplemented with protease and phosphatase inhibitor cocktail (Roche, Basel, Switzerland). Equal amounts of protein (30 μ g) were loaded to SDS-PAGE and transferred to nitrocellulose membrane After blocking with 1% ROTI®Block (Carl Roth, Karlsruhe, Germany) or 5% dry milk in TBS/T, blots were incubated with primary antibodies against insulin (1:1000, STJ24210; St John's Laboratory, London, United Kingdom), glucagon (1:500, PA5-13442; Thermo Fisher Scientific), somatostatin (1:2000, STJ95730; St John's Laboratory), GLUT2 (1:4000, 07-1402, Merck Millipore, Burlington, USA), and GAPDH (1:1000, 3686, Cell Signaling Technology, Boston, USA). Followed by an incubation with HRP-conjugated secondary antibody, immunoreactions were detected by visualizing the peroxidase activity with an ECL Kit (Pierce™ ECL Western Blotting Substrate, Thermo Fisher Scientific). For reloading the membrane with primary antibody, blots were stripped with western blot stripping buffer (Thermo Fisher Scientific) according to the manufacturer's instruction.

Statistical analysis

Data are presented as means \pm SEM and as column bar graphs or as pie charts of at least three animals evaluated by the Student's *t*-test, or the Mann-Whitney U test as calculated by GraphPad Prism (GraphPad Software, La Jolla, CA). A *p*-value < 0.05 was considered statistically significant.

Acknowledgments: This work is funded by the Deutsche Forschungsgemeinschaft (DFG, German Research Foundation) – Projektnummer 209933838 – SFB 1052 (project B09). Martin Gericke is the recipient of this funding. We thank Kathrin Jäger and Andreas Lösche from the FACS core unit and Michaela Kirstein (MLU Halle) for technical assistance. Further, we thank Juliane Zibolka and Ivonne Bazwinsky-Wutschke (MLU Halle) for help with establishing Western Blot analyses.

Open access funding enabled and organized by Projekt DEAL.

Author contributions: M.G. and I.B. designed the study. G.B. carried out the experiments with help from J.F. (ITT/GTT) and L.A. (ELISA, Western Blot), J.B. (qPCR; FACS), C.H. (genotyping), and A.L. (immunofluorescence analyses). G.B. analyzed the data with help from J.F. and M.G. G.B. drafted and M.G. and I.B. revised the paper. All authors approved the final version of the manuscript.

Conflict of interest: The authors declare no financial or commercial conflict of interest.

Peer review: The peer review history for this article is available at <https://publons.com/publon/10.1002/eji.202048870>

Data availability statement: The data that support the findings of this study are available from the corresponding author upon reasonable request.

References

- James, W. P. T., WHO recognition of the global obesity epidemic. *Int. J. Obes.* (2005) 2008. 32: S120–6.
- Economic costs of diabetes in the U.S. in 2017. *Diabetes Care.* 2018. 41: 917–928.
- Weisberg, S. P., McCann, D., Desai, M., Rosenbaum, M., Leibel, R. L. and Ferrante, A. W., Obesity is associated with macrophage accumulation in adipose tissue. *J. Clin. Invest.* 2003. 112: 1796–1808.
- Winer, D. A., Winer, S., Shen, L., Wadia, P. P., Yantha, J., Paltser, G., Tsui, H. et al., B cells promote insulin resistance through modulation of T cells and production of pathogenic IgG antibodies. *Nat. Med.* 2011. 17: 610–617.
- Winer, S., Chan, Y., Paltser, G., Truong, D., Tsui, H., Bahrami, J., Dorfman, R. et al., Normalization of obesity-associated insulin resistance through immunotherapy. *Nat. Med.* 2009. 15: 921–929.

- 6 Liu, J., Divoux, A., Sun, J., Zhang, J., Clément, K., Glickman, J. N., Sukhova, G. K. et al., Genetic deficiency and pharmacological stabilization of mast cells reduce diet-induced obesity and diabetes in mice. *Nat. Med.* 2009. 15: 940–945.
- 7 Talukdar, S., Oh, D. Y., Bandyopadhyay, G., Li, D., Xu, J., McNelis, J., Lu, M. et al., Neutrophils mediate insulin resistance in mice fed a high-fat diet through secreted elastase. *Nat. Med.* 2012. 18: 1407–1412.
- 8 O'Rourke, R. W., Metcalf, M. D., White, A. E., Madala, A., Winters, B. R., Maizlin, I. I., Jobe, B. A. et al., Depot-specific differences in inflammatory mediators and a role for NK cells and IFN-gamma in inflammation in human adipose tissue. *Int. J. Obes. (2005)* 2009. 33: 978–990.
- 9 Gastaldelli, A., Miyazaki, Y., Pettiti, M., Matsuda, M., Mahankali, S., Santini, E., DeFronzo, R. A. et al., Metabolic effects of visceral fat accumulation in type 2 diabetes. *J. Clin. Endocrinol. Metab.* 2002. 87: 5098–5103.
- 10 Klötting, N., Fasshauer, M., Dietrich, A., Kovacs, P., Schön, M. R., Kern, M., Stumvoll, M. et al., Insulin-sensitive obesity. *Am. J. Physiol. Endocrinol. Metab.* 2010. 299: E506–515.
- 11 Cho, K. W., Morris, D. L. and Lumeng, C. N., Flow cytometry analyses of adipose tissue macrophages. *Methods Enzymol.* 2014. 537: 297–314.
- 12 Martinez, F. O. and Gordon, S., The M1 and M2 paradigm of macrophage activation: time for reassessment. *F1000Prime Reports* 2014. 6: 13.
- 13 Lumeng, C. N., Bodzin, J. L. and Saltiel, A. R., Obesity induces a phenotypic switch in adipose tissue macrophage polarization. *J. Clin. Invest.* 2007. 117: 175–184.
- 14 Zheng, C., Yang, Q., Cao, J., Xie, N., Liu, K., Shou, P., Qian, F. et al., Local proliferation initiates macrophage accumulation in adipose tissue during obesity. *Cell Death. Dis.* 2016. 7: e2167.
- 15 Bourlier, V., Zakaroff-Girard, A., Miranville, A., de Barros, S., Maumus, M., Sengenès, C., Galitzky, J. et al., Remodeling phenotype of human subcutaneous adipose tissue macrophages. *Circulation* 2008. 117: 806–815.
- 16 Amano, S. U., Cohen, J. L., Vangala, P., Tencerova, M., Nicoloso, S. M., Yawe, J. C., Shen, Y. et al., Local proliferation of macrophages contributes to obesity-associated adipose tissue inflammation. *Cell Metab.* 2014. 19: 162–171.
- 17 Haase, J., Weyer, U., Immig, K., Klötting, N., Blüher, M., Eilers, J., Bechmann, I. et al., Local proliferation of macrophages in adipose tissue during obesity-induced inflammation. *Diabetologia* 2014. 57: 562–571.
- 18 Braune, J., Weyer, U., Hobusch, C., Mauer, J., Brüning, J. C., Bechmann, I. and Gericke, M., IL-6 Regulates M2 polarization and local proliferation of adipose tissue macrophages in obesity. *J. Immunol. (Baltimore, Md. 1950)* 2017. 198: 2927–2934.
- 19 Tardelli, M., Zeyda, K., Moreno-Viedma, V., Wanko, B., Grün, N. G., Staffler, G., Zeyda, M. et al., Osteopontin is a key player for local adipose tissue macrophage proliferation in obesity. *Mol. Metabol.* 2016. 5: 1131–1137.
- 20 Shirakawa, K., Yan, X., Shinmura, K., Endo, J., Kataoka, M., Katsumata, Y., Yamamoto, T. et al., Obesity accelerates T cell senescence in murine visceral adipose tissue. *J. Clin. Invest.* 2016. 126: 4626–4639.
- 21 Osborn, O. and Olefsky, J. M., The cellular and signaling networks linking the immune system and metabolism in disease. *Nat. Med.* 2012. 18: 363–374.
- 22 Nishimura, S., Manabe, I., Nagasaki, M., Eto, K., Yamashita, H., Ohsugi, M., Otsu, M. et al., CD8⁺ effector T cells contribute to macrophage recruitment and adipose tissue inflammation in obesity. *Nat. Med.* 2009. 15: 914–920.
- 23 Feuerer, M., Herrero, L., Cipolletta, D., Naaz, A., Wong, J., Nayer, A., Lee, J. et al., Lean, but not obese, fat is enriched for a unique population of regulatory T cells that affect metabolic parameters. *Nat. Med.* 2009. 15: 930–939.
- 24 Zeng, Q., Sun, X., Xiao, L., Xie, Z., Bettini, M. and Deng, T., A unique population: adipose-resident regulatory T cells. *Front. Immunol.* 2018. 9: 2075.
- 25 Vasanthakumar, A., Moro, K., Xin, A., Liao, Y., Gloury, R., Kawamoto, S., Fagarasan, S. et al., The transcriptional regulators IRF4, BATF and IL-33 orchestrate development and maintenance of adipose tissue-resident regulatory T cells. *Nat. Immunol.* 2015. 16: 276–285.
- 26 Han, J. M., Wu, D., Denroche, H. C., Yao, Y., Verchere, C. B. and Levings, M. K., IL-33 reverses an obesity-induced deficit in visceral adipose tissue ST2⁺ T regulatory cells and ameliorates adipose tissue inflammation and insulin resistance. *J. Immunol. (Baltimore, Md. 1950)*. 2015. 194: 4777–4783.
- 27 Li, C., DiSpirito, J. R., Zemmour, D., Spallanzani, R. G., Kuswanto, W., Benoist, C. and Mathis, D., TCR transgenic mice reveal stepwise, multi-site acquisition of the distinctive fat-treg phenotype. *Cell* 2018. 174: 285–299.e12.
- 28 Deng, T., Liu, J., Deng, Y., Minze, L., Xiao, X., Wright, V., Yu, R. et al., Adipocyte adaptive immunity mediates diet-induced adipose inflammation and insulin resistance by decreasing adipose Treg cells. *Nat. Commun.* 2017. 8: 1–11.
- 29 Cipolletta, D., Feuerer, M., Li, A., Kamei, N., Lee, J., Shoelson, S. E., Benoist, C. et al., PPAR- γ is a major driver of the accumulation and phenotype of adipose tissue Treg cells. *Nature* 2012. 486: 549–553.
- 30 Bapat, S. P., Myoung Suh, J., Fang, S., Liu, S., Zhang, Y., Cheng, A., Zhou, C. et al., Depletion of fat-resident Treg cells prevents age-associated insulin resistance. *Nature* 2015. 528: 137–141.
- 31 Strissel, K. J., DeFuria, J., Shaul, M. E., Bennett, G., Greenberg, A. S. and Obin, M. S., T-cell recruitment and Th1 polarization in adipose tissue during diet-induced obesity in C57BL/6 mice. *Obesity (Silver Spring, Md.)* 2010. 18: 1918–1925.
- 32 Cipolletta, D., Cohen, P., Spiegelman, B. M., Benoist, C. and Mathis, D., Appearance and disappearance of the mRNA signature characteristic of Treg cells in visceral adipose tissue: Age, diet, and PPAR γ effects. *PNAS* 2015. 112: 482–487.
- 33 Han, J. M., Wu, D., Denroche, H. C., Yao, Y., Verchere, C. B. and Levings, M. K., IL-33 reverses an obesity-induced deficit in visceral adipose tissue ST2⁺ T regulatory cells and ameliorates adipose tissue inflammation and insulin resistance. *J. Immunol. (Baltimore, Md. 1950)*. 2015. 194: 4777–4783.
- 34 Miller, A. M., Asquith, D. L., Hueber, A. J., Anderson, L. A., Holmes, W. M., McKenzie, A. N., Xu, D. et al., Interleukin-33 induces protective effects in adipose tissue inflammation during obesity in mice. *Circ. Res.* 2010. 107: 650–658.
- 35 Eller, K., Kirsch, A., Wolf, A. M., Sopper, S., Tagwerker, A., Stanzl, U., Wolf, D. et al., Potential role of regulatory T cells in reversing obesity-linked insulin resistance and diabetic nephropathy. *Diabetes* 2011. 60: 2954–2962.
- 36 Deng, T., Lyon, C. J., Minze, L. J., Lin, J., Zou, J., Liu, J. Z., Ren, Y. et al., Class II major histocompatibility complex plays an essential role in obesity-induced adipose inflammation. *Cell Metab.* 2013. 17: 411–422.
- 37 Kintscher, U., Hartge, M., Hess, K., Foryst-Ludwig, A., Clemenz, M., Wabitsch, M., Fischer-Posovszky, P. et al., T-lymphocyte infiltration in visceral adipose tissue: a primary event in adipose tissue inflammation and the development of obesity-mediated insulin resistance. *Arterioscler. Thromb. Vasc. Biol.* 2008. 28: 1304–1310.
- 38 Zamarron, B. F., Mergian, T. A., Cho, K. W., Martinez-Santibanez, G., Luan, D., Singer, K., DelProposto, J. L. et al., Macrophage proliferation sustains adipose tissue inflammation in formerly obese mice. *Diabetes* 2017. 66: 392–406.
- 39 Ferran, C., Sheehan, K., Dy, M., Schreiber, R., Merite, S., Landais, P., Noel, L. H. et al., Cytokine-related syndrome following injection of anti-CD3 monoclonal antibody: further evidence for transient in vivo T cell activation. *Eur. J. Immunol.* 1990. 20: 509–515.

- 40 Ferran, C., Dy, M., Sheehan, K., Merite, S., Schreiber, R., Landais, P., Grau, G. et al., Inter-mouse strain differences in the in vivo anti-CD3 induced cytokine release. *Clin. Exp. Immunol.* 1991. **86**: 537–543.
- 41 Alegre, M., Vandenabeele, P., Flamand, V., Moser, M., Leo, O., Abramowicz, D., Urbain, J. et al., Hypothermia and hypoglycemia induced by anti-CD3 monoclonal antibody in mice: role of tumor necrosis factor. *Eur. J. Immunol.* 1990. **20**: 707–710.
- 42 Vossen, A. C., Tibbe, G. J., Kroos, M. J., van de Winkel, J. G., Benner, R. and Savelkoul, H. F., Fc receptor binding of anti-CD3 monoclonal antibodies is not essential for immunosuppression, but triggers cytokine-related side effects. *Eur. J. Immunol.* 1995. **25**: 1492–1496.
- 43 Vossen, A. C., Knulst, A. C., Tibbe, G. J., van Oudenaren, A., Baert, M. R., Benner, R. and Savelkoul, H. F., Suppression of skin allograft rejection in mice by anti-CD3 monoclonal antibodies without cytokine-related side-effects. *Transplantation* 1994. **58**: 257–261.
- 44 Roat, R., Rao, V., Doliba, N. M., Matschinsky, F. M., Tobias, J. W., Garcia, E., Ahima, R. S. et al., Alterations of pancreatic islet structure, metabolism and gene expression in diet-induced obese C57BL/6J mice. *PLoS One* 2014. **9**: e86815.
- 45 Müller, W. A., Faloona, G. R., Aguilar-Parada, E. and Unger, R. H., Abnormal alpha-cell function in diabetes. Response to carbohydrate and protein ingestion. *N. Eng. J. Med.* 1970. **283**: 109–115.
- 46 Gromada, J., Chabosseau, P. and Rutter, G. A., The α -cell in diabetes mellitus. *Nat. Rev. Endocrinol.* 2018. **14**: 694–704.
- 47 Newgard, C. B., An, J., Bain, J. R., Muehlbauer, M. J., Stevens, R. D., Lien, L. F., Haqq, A. M. et al., A branched-chain amino acid-related metabolic signature that differentiates obese and lean humans and contributes to insulin resistance. *Cell Metab.* 2009. **9**: 311–326.
- 48 Stern, J. H., Smith, G. I., Chen, S., Unger, R. H., Klein, S. and Scherer, P. E., Obesity dysregulates fasting-induced changes in glucagon secretion. *J. Endocrinol.* 2019. **243**: 149–160.
- 49 Knop, F. K., Aaboe, K., Vilsbøll, T., Vølund, A., Holst, J. J., Krarup, T. and Madsbad, S., Impaired incretin effect and fasting hyperglucagonaemia characterizing type 2 diabetic subjects are early signs of dysmetabolism in obesity. *Diabetes Obes. Metab.* 2012. **14**: 500–510.
- 50 Kellard, J. A., Rorsman, N. J. G., Hill, T. G., Armour, S. L., van de Bunt, M., Rorsman, P., Knudsen, J. G. and Briant, L. J. B., Reduced somatostatin signalling leads to hypersecretion of glucagon in mice fed a high-fat diet. *Mol. Metab.* 2020. **40**: 101021.
- 51 Bagger, J. I., Knop, F. K., Lund, A., Holst, J. J. and Vilsbøll, T., Glucagon responses to increasing oral loads of glucose and corresponding isoglycaemic intravenous glucose infusions in patients with type 2 diabetes and healthy individuals. *Diabetologia* 2014. **57**: 1720–1725.
- 52 Wagner, R., Hakaste, L. H., Ahlqvist, E., Heni, M., Machann, J., Schick, F., van Obberghen, E. et al., Nonsuppressed glucagon after glucose challenge as a potential predictor for glucose tolerance. *Diabetes* 2017. **66**: 1373–1379.
- 53 Merino, B., Alonso-Magdalená, P., Lluésma, M., Neco, P., Gonzalez, A., Marroquí, L., García-Arévalo, M. et al., Pancreatic alpha-cells from female mice undergo morphofunctional changes during compensatory adaptations of the endocrine pancreas to diet-induced obesity. *Sci. Rep.* 2015. **5**: 11622.
- 54 Hædersdal, S., Lund, A., Knop, F. K. and Vilsbøll, T., The role of glucagon in the pathophysiology and treatment of Type 2 diabetes. *Mayo Clin. Proc.* 2018. **93**: 217–239.
- 55 Strowski, M. Z., Parmar, R. M., Blake, A. D. and Schaeffer, J. M., Somatostatin inhibits insulin and glucagon secretion via two receptors subtypes: an in vitro study of pancreatic islets from somatostatin receptor 2 knock-out mice. *Endocrinology* 2000. **141**: 111–117.
- 56 Omar-Hmeadi, M., Lund, P.-E., Gandasi, N. R., Tengholm, A. and Barg, S., Paracrine control of α -cell glucagon exocytosis is compromised in human type-2 diabetes. *Nat. Commun.* 2020. **11**: 1896.
- 57 Sasmono, R. T., Oceandy, D., Pollard, J. W., Tong, W., Pavli, P., Wainwright, B. J., Ostrowski, M. C. et al., A macrophage colony-stimulating factor receptor-green fluorescent protein transgene is expressed throughout the mononuclear phagocyte system of the mouse. *Blood* 2003. **101**: 1155–1163.
- 58 Orthgiess, J., Gericke, M., Immig, K., Schulz, A., Hirrlinger, J., Bechmann, I. and Eilers, J., Neurons exhibit *Lyz2* promoter activity in vivo: Implications for using *LysM-Cre* mice in myeloid cell research. *Eur. J. Immunol.* 2016. **46**: 1529–1532.
- 59 Gericke, M., Weyer, U., Braune, J., Bechmann, I. and Eilers, J., A method for long-term live imaging of tissue macrophages in adipose tissue explants. *Am. J. Physiol. Endocrinol. Metab.* 2015. **308**: E1023–33.
- 60 Cinti, S., Mitchell, G., Barbatelli, G., Murano, I., Ceresi, E., Faloia, E., Wang, S. et al., Adipocyte death defines macrophage localization and function in adipose tissue of obese mice and humans. *J. Lipid Res.* 2005. **46**: 2347–2355.
- 61 Strissel, K. J., Stancheva, Z., Miyoshi, H., Perfield, J. W., DeFuria, J., Jick, Z., Greenberg, A. S. et al., Adipocyte death, adipose tissue remodeling, and obesity complications. *Diabetes* 2007. **56**: 2910–2918.
- 62 Cossarizza, A., Chang, H.-D., Radbruch, A., Akdis, M., Andrä, I., Annunziato, F., Bacher, P. et al., Guidelines for the use of flow cytometry and cell sorting in immunological studies. *Eur. J. Immunol.* 2017. **47**: 1584–1797.
- 63 Bustin, S. A. (Ed.) *A - Z of quantitative PCR*. Internat. Univ. Line, La Jolla, Calif. 2004.
- 64 Zibolka, J., Wolf, A., Rieger, L., Rothgänger, C., Jörns, A., Lutz, B., Zimmer, A. et al., Influence of cannabinoid receptor deficiency on parameters involved in blood glucose regulation in mice. *Int. J. Mol. Sci.* 2020. **21**.

Abbreviations: **AT:** adipose tissue · **ATL:** adipose tissue lymphocyte · **ATM:** adipose tissue macrophage · **BrdU:** bromodeoxyuridine · **CLS:** crown-like structure · **FOXP3:** Forkhead box P3 · **GTT:** glucose tolerance testing · **HFD:** high-fat diet · **ITT:** insulin tolerance testing · **NCD:** normal chow diet · **OPN:** osteopontin · **PCNA:** proliferating cell nuclear antigen · **Treg:** regulatory T cell · **ST2:** suppression of tumorigenicity 2 · **TH2 cell:** T helper type 2 cell · **VAT:** visceral adipose tissue

Full correspondence: Prof. Martin Gericke, Institute of Anatomy and Cell Biology, Martin-Luther-University Halle-Wittenberg, Grosse Steinstrasse 52, D-06108 Halle (Saale), Germany
e-mail: martin.gericke@medizin.uni-halle.de
Fax: +49 345 557 1700

Received: 13/7/2020

Revised: 10/2/2021

Accepted: 16/3/2021

Accepted article online: 30/3/2021